Absence of Fluid-Ordered/Fluid-Disordered Phase Coexistence in Ceramide/POPC Mixtures Containing Cholesterol

M. Fidorra,*[†] L. Duelund,*[‡] C. Leidy,[¶] A. C. Simonsen,*[†] and L.A. Bagatolli*[§]

*MEMPHYS-Center for Biomembrane Physics, [†]Department of Physics, [‡]Department of Chemistry, and [§]Department of Biochemistry and Molecular Biology, University of Southern Denmark, Odense, Denmark; and [¶]Department of Physics, Universidad de los Andes, Bogotá, Colombia

ABSTRACT   The effect of temperature on the lateral structure of lipid bilayers composed of porcine brain ceramide and 1-palmitoyl 2-oleoyl-phosphatidylcholine (POPC), with and without addition of cholesterol, were studied using differential scanning calorimetry, Fourier transformed infrared spectroscopy, atomic force microscopy, and confocal/two-photon excitation fluorescence microscopy (which included LAURDAN generalized polarization function images). A broad gel/fluid phase coexistence temperature regime, characterized by the presence of micrometer-sized gel-phase domains with stripe and flowerlike shapes, was observed for different POPC/ceramide mixtures (up to ~25 mol % ceramide). This observed phase coexistence scenario is in contrast to that reported previously for this mixture, where absence of gel/fluid phase coexistence was claimed using bulk LAURDAN generalized polarization (GP) measurements. We demonstrate that this apparent discrepancy (based on the direct comparison between the LAURDAN GP data obtained in the microscope and the fluorometer) disappears when the additive property of the LAURDAN GP function is taken into account to examine the data obtained using bulk fluorescence measurements. Addition of cholesterol to the POPC/ceramide mixtures shows a gradual transition from a gel/fluid to gel/liquid-ordered phase coexistence scenario as indicated by the different experimental techniques used in our experiments. This last result suggests the absence of fluid-ordered/fluid-disordered phase coexistence in the ternary mixtures studied in contrast to that observed at similar molar concentrations with other ceramide-base-containing lipid mixtures (such as POPC/sphingomyelin/cholesterol, which is used as a canonical raft model membrane). Additionally, we observe a critical cholesterol concentration in the ternary mixtures that generates a peculiar lateral pattern characterized by the observation of three distinct regions in the membrane.

INTRODUCTION

Ceramides have been postulated to have important structural and functional roles in membrane-related biological processes. It has been reported, for example, that ceramide molecules are membrane-associated second messenger molecules, participating in processes that occur during cell growth (differentiation) and cell aging (apoptosis) (1,2). Ceramides molecules are also natural constituents of skin, having an important role in determining the particular physical properties of the barrier-forming intercellular lamellae found in the outermost layer of the epidermis (3–5). Due to their particular chemical structure, which is characterized by a very small headgroup, self-assembling ceramide structures display strong intermolecular interactions (mainly hydrogen bonds) and a very high order-disorder phase transition temperature, well above physiological temperatures (6). Ceramides, together with other ceramide-based lipids such as sphingomyelin and various glycosphingolipids and also DPPC, are some of the few naturally occurring membrane lipids that display lipid phase transition temperatures

above physiological temperatures (7,8). The very particular geometrical features of the ceramide molecule (that promote in some cases formation of nonlamellar phases (9,10)) allow this lipid to be a strong regulator of the lateral structure of biological membranes. For example, production of ceramide from sphingomyelin (SM), by the action of sphingomyelinases, produces changes in lipid lateral distribution and membrane morphology of SM/SOPC giant vesicles upon ceramide formation (11). Sphingomyelinase activation appears to be at the origin of many cell signaling events (1,12–14) in which changes in membrane structure induced by the production of ceramide are believed to play a key regulatory role. Additionally, ceramide-induced membrane permeability in isolated mitochondria was reported to be a result of the formation of ceramide channels (15,16). It has also been claimed that ceramide participates in the formation of specialized membrane regions (lipid rafts) by stabilizing sphingomyelin-enriched domains (17) and displacing cholesterol from the fluid-ordered domains (18).

Studies regarding the thermotropic behavior of ceramide/ phospholipid mixtures were reported from different laboratories (19–22). In particular, different results were observed using POPC/ceramide mixtures based on different experimental techniques. For example, Massey (22) concludes that ceramide-rich domains do not form in POPC/brain ceramide mixtures based on fluorescent probe bulk measurements (using LAURDAN and DPH), attributing this result to the

similarity in the fatty-acid chain length between the lipid species. On the other hand, Hsueh et al. (21), exploring palmitoyl-ceramide/POPC mixtures, claim the existence of palmitoyl ceramide-rich domains in a broad temperature range using deuterium NMR. To gain further information on the particular lateral structure of these ceramide-containing membranes, we studied POPC/brain ceramide mixtures and compared our results with the previous observations done in the aforementioned POPC-containing mixtures (21,22). In our experiments, dynamical and structural information obtained by direct visualization of single vesicles (using confocal and two-photon excitation fluorescence microscopy) or planar membranes (using atomic force microscopy) is related to bulk physical measurements obtained from liposome-solution experiments (using differential scanning calorimetry and infrared and fluorescence spectroscopy). This combination allows us to correlate membrane morphological details (such as lipid domain size and shape) with the membrane physical characteristics at a molecular level (23,24). Finally, the effect of cholesterol on the lateral structure of POPC/ceramide mixtures was explored using the same experimental approach and compared with previously reported results obtained for other ternary mixtures containing ceramide-based lipids such as the canonical raft mixture POPC/SM/cholesterol (25). Our results indicate a clear difference in the behavior of the lipid domain structure as a function of cholesterol concentration for membranes containing ceramide compared to those containing sphingomyelin.

MATERIALS AND METHODS

1-Palmitoyl 2-oleoyl-phosphatidylcholine (POPC), deuterated 1-palmitoyl 2-oleoyl-phosphatidylcholine (POPC-d31), ceramide (porcine brain), and cholesterol were purchased from Avanti Polar Lipids (Alabaster, AL). Porcine brain ceramide is a complex mixture of different ceramides containing a variety of fatty acid species (saturated and unsaturated). For instance, 50% of the ceramide species correspond to the saturated stearoyl-ceramide and 35% of the ceramide species have hydrophobic chains of more than 22 carbons (20% of the total population correspond to the unsaturated 24:1 ceramide species). Ergosterol was purchased from Fluka (Copenhagen, Denmark). 6-Lauroyl-2-(n,n-dimethylamino)naphthalene (LAURDAN) and 1,1′-dioctadecyl-3,3,3′,3′-tetramethylindocarbocyanine perchlorate (DiI$_{C18}$) were purchased from Molecular Probes (Invitrogen, Copenhagen, Denmark).

Vesicle preparation

Giant unilamellar vesicles

Giant unilamellar vesicles (GUVs) were obtained by the electroformation method originally described by Angelova (26). The vesicles were electroformed using Indium thin oxide (ITO) planar electrodes (Thin Film Devices, Anaheim, CA) or Pt wire electrodes in special chambers described in Fig. 1. In the case of ITO planar electrodes, an aliquot of the desired lipid mixture containing the fluorescent probe (<0.5 mol %) dissolved in organic solvent (Cl$_3$CH/MetOH 2:1 v/v) was deposited on the electrode surface using the spin-coating technique (50 μl of 3 mg/ml lipid stock solution at 3000 rpm (27)) or simply by adding the desired amount of the lipid organic solution with subsequent solvent evaporation at room temperature (6 μl of 1mg/ml lipid stock solution in trifluoroethanol). In the case of the Pt electrodes, the
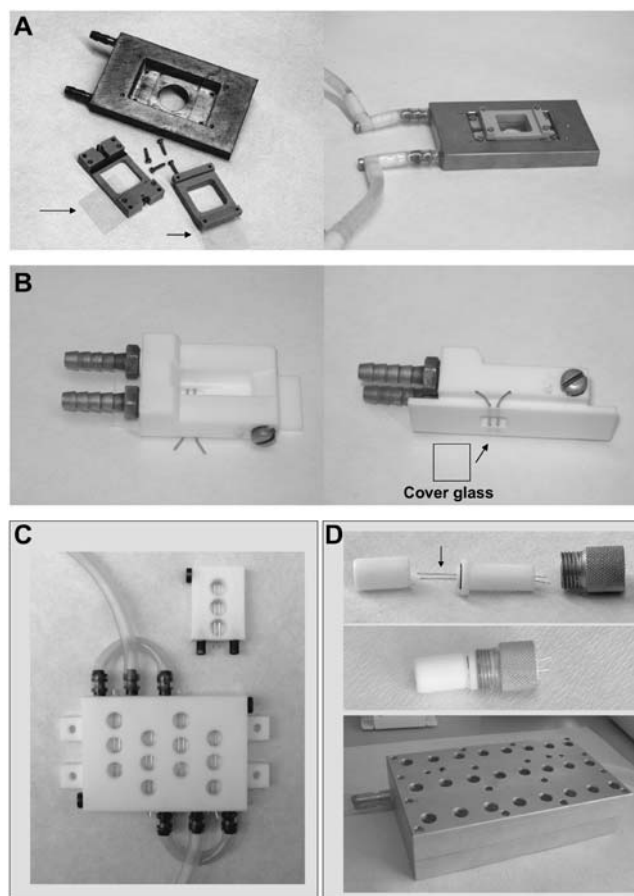

FIGURE 1 Special chambers to prepare GUVs using the electroformation method (described in Materials and Methods). (A) Chamber to generate GUVs using planar ITO electrodes (standard cover glasses 22 × 22 mm, with one of the surfaces covered with a transparent ITO layer). The arrows indicate the ITO electrode plastic supports, together with the ITO electrodes. The distance between electrode surfaces is 3 mm. The metal piece shown in the figure has a water circulation path to maintain the sample at the desired temperature. This unit is mounted in the microscope stage and the vesicles are prepared in the microscope (to follow, in situ, the formation process of the GUVs). (B) Chamber to generate GUVs using cylindrical Pt electrodes (diameter 1 mm, also works very well with 0.5-mm diameter Pt wires). The dimensions of the bottom of the chamber correspond to a standard microscope slide. The distance center-to-center of the Pt electrodes is 3 mm. The distance from the bottom of the coverglass (glued with epoxy J-B KWIK, J-B Weld, Sulfur Springs, TX) to the surface of the electrodes, in this case, is 100 μl (this would depend on the microscope objective's working distance used to perform the experiments). (C) Array of individual chamber (×3 and ×12). The volume of each chamber is 600 μl. The Pt wires diameter is 1 mm. (D) Array of individual chamber (×24). The Teflon lid allows closing the chamber (without having significant evaporation) and attaching it to the metal piece, which is heated using water. The temperature range for GUV preparation is from 3 up to 98°C. The Pt wires have a diameter of 0.5 mm; distance between electrodes, center to center, is 3 mm.

same lipid mixtures were deposited on the Pt surface (3 μl of a 0.2 mg/ml lipid stock solution in Cl$_3$CH in each electrode). After this procedure, the sample was placed overnight under vacuum to remove traces of the organic solvent (for both the planar ITO and the Pt electrode). After this last step sufficient amounts of MilliQ water (17.5 MΩ; Millipore, Billerica, MA) were added to the ITO or the Pt electrodes and a low frequency AC field was

applied in all cases using a function generator (Vann Draper Digimess Fg 100, Stenson, Derby, UK; sine function, freq. 10 Hz, amplitude 2 V) for 1–2 h. The temperature used for GUV formation was well above the fluid/gel phase transition temperature (~80°C for all samples). One of the advantages of these chambers (see Fig. 1, A and B) is the fact that vesicle formation can be directly observed in the microscope. In this last case, the vesicles remain adsorbed onto the electrode surface, and remain immobile. Alternatively, the vesicles prepared in the chamber indicated in Fig. 1, C and D, were electroformed using sucrose solution 200 mOsM. In these chambers, it is not possible to monitor vesicle formation under the microscope. In this case, after vesicle formation, the AC field was turned off and the vesicles were transferred to an iso-osmolar glucose solution in a special chamber (200 μl of glucose + 50 μl of the GUVs in sucrose in each of the eight wells of the plastic chamber used; LabTek, Naperville, IL). The density difference between the interior and exterior of the GUVs induces the vesicles to sink to the bottom of the chamber and within a few minutes the vesicles are ready to be observed using an inverted microscope. The temperature in this last case is controlled by a homebuilt unit by using a commercial water-bath heater. It is important to mention that in some cases, the GUVs, which have sunk to the glass surface, can move during image acquisition (in particular, when three-dimensional images are acquired at high temperatures), a disadvantage with respect to the use of the alternative chambers where the vesicles are adsorbed to the electrode and show practically no mobility. Importantly, no significant differences were observed among the samples obtained using the five different chambers. In addition, it is important to point out that formation of giant vesicles above 30 mol % of ceramide was very difficult to perform. At high ceramide concentration the inability to form GUVs is likely due to either incomplete hydration of the ceramides or the formation of nonlamellar phases.

Multilamellar vesicles

Multilamellar vesicles (MLVs) were prepared by drying the organic solvent from a proper amount of lipid stock solution under a stream of N_2. To remove potential traces of organic solvent the dried samples were placed under vacuum for 3 h. The tubes containing the dried lipid solutions were then hydrated using MilliQ water or buffer (20 mM TrisClH-50 mM NaCl, pH 7.4) at 90°C for 30 min (no differences were observed between these two preparations). During this incubation time the lipid solutions were agitated every 5 min, resulting in a turbid solution. After this last procedure, the vesicles were placed in an oven at 55°C overnight and agitated again before proceeding with the experiments. In the case of the LAURDAN experiments, the probe was premixed with the lipids in a ratio corresponding to a 1:200 mol fraction (LAURDAN final concentration was 1 μM).

Fluorescence microscopy experiments

An inverted confocal/two-photon excitation fluorescence microscope (Zeiss model No. LSM 510 META NLO; Carl Zeiss, Jena, Germany) and a previously described homebuilt, two-photon excitation microscope exclusively used to obtain the LAURDAN generalized polarization (GP) images (28–31), were used in our experiments. The Zeiss-LSM 510 META NLO microscope was used to obtain combined LAURDAN and DiI$_{C18}$ fluorescent images. This type of measurement is important for obtaining a spatial correlation between the particular locations of the two fluorescent probes in the lipid membrane. In this last experiment, the excitation wavelengths were 543 nm (for DiI$_{C18}$ in one photon excitation mode) and 780 nm (for LAURDAN in two-photon excitation mode) and the fluorescence signals were simultaneously collected in two different channels using bandpass filters of 590 ± 25 nm and 424 ± 37 nm (for DiI$_{C18}$ and LAURDAN, respectively). For the Zeiss-LSM 510 META NLO microscope, the Ti:Sa laser used for two-photon excitation mode was a MaiTai XF-W2S (Broadband MaiTai with 10 W Millennia pump laser, tunable excitation range 710–980 nm; Spectra Physics, Mountain View, CA). The objectives used for the experiments were a 40× water immersion, NA 1.2, and a 20×

air objective, NA 0.75. In particular, the 20× air objective was used in the temperature scan experiments. The use of water or oil immersion objectives at high temperature is not recommended (our temperature scan started at 60°C) because the objectives can be easily damaged at such conditions. The GUV's fluorescent images were obtained either at the polar region of the GUVs, i.e., the north or south pole of the vesicle (the circumpolar region), or the equatorial region of the vesicle. In this article, we use the terms ''polar region'' and ''equatorial region'' to refer to these two different situations (see *inset* in Fig. 11).

LAURDAN GP measurements

The LAURDAN GP measurement denotes the position of the probe's emission spectra (32). The fluorescence emission properties of LAURDAN are sensitive to the water dipolar relaxation process that occurs in the probe's local environment (in this case, the lipid bilayer). The extent of water dipolar relaxation observed in the gel phase is very low compared to what is observed in the fluid phase (high extent of water dipolar relaxation process). As a consequence the probe's emission is blue in the gel phase and green in the fluid phase (32). The GP function was defined analogously to the fluorescence polarization function as

$$GP = \frac{I_B - I_R}{I_B + I_R}, \qquad (1)$$

where I_B and I_R correspond to the intensities at the blue and red edges of the emission spectrum (respectively) using a given excitation wavelength (32–34). Consequently, the LAURDAN GP is related to the lateral packing of the lipid bilayers (32). High LAURDAN GP values (0.5–0.6) correspond to laterally ordered, gel-like phases, whereas low LAURDAN GP values (below 0) correspond to fluid phases.

To measure the GP of the LAURDAN-labeled multilamellar vesicles (bulk measurements), a Chronos ISS fluorometer (ISS, Champaign, IL) was used. The excitation wavelength was 374 nm (using a laser diode as excitation source). The emission wavelengths were 440 nm for the I_B and 490 for the I_R (Eq. 1). As was stated in the previous section, the two-photon excitation LAURDAN generalized polarization (GP) images were obtained using a homebuilt, two-photon excitation fluorescence microscope (28–31). The LAURDAN GP images were computed using fluorescence intensity images obtained simultaneously in the blue and red regions of the probe emission spectra (bandpass filters 446 ± 23 nm and 499 ± 23 nm), using 780 nm as excitation wavelength (31). The objective used was a long working distance 20× air objective, NA 0.75.

LAURDAN photoselection effect

The lack of fluorescence in the gel phase domains due to the well-described photoselection effect (23,24,35) was observed in the LAURDAN fluorescence images obtained at the polar region of the GUVs. This phenomenon was used as a qualitative criterion to complement the information obtained from the shift in LAURDAN's emission spectrum (24,25,29,30,35). Particularly, the photoselection effect is related to the probe orientation in the lipid membrane and is used in our experiments to gain further information about the lateral packing features of particular regions of the lipid membrane (36,37).

Atomic force microscopy (AFM) experiments

Freshly cleaved muscovite mica (Plano, Wetzlar, Germany), with a size of 8 × 8 mm^2, was used for preparing supported membranes. The preparation was done by using a spin-coating protocol as described previously (27), with lipid mixtures containing 0.7% DiI$_{C18}$. Briefly, the spin-coating protocol consists of placing a 20-μl droplet of lipid in a hexane/methanol (97:3) solution onto the mica support and immediately thereafter spinning the sample to 3000 rpm for 40 s while the solvent evaporates. A Chemat KW-4A

spin-coater (Chemat, Northridge, CA) was used for the coating process. After overnight storage under vacuum, the sample was hydrated in MilliQ water and annealed to 65°C for 1 h to yield a single and highly uniform supported membrane. Excess lipid was removed by washing with fresh MilliQ water (at 65°C) and the effect of the washing was monitored continuously. Epi-fluorescence microscopy of the supported membrane was performed with the sample placed in a microscope chamber (LabTek) on a Nikon TE2000 inverted microscope (Nikon, Badhoevedorp, The Netherlands), using a 40× long working distance (ELWD) objective. Fluorescence excitation was done with a halogen lamp and using a G-2A filtercube (Nikon) and fluorescence images were recorded with a Coolsnap CF camera (Photometrics, Tucson, AZ). The samples were measured with the atomic force microscope using a PicoSPM (Molecular Imaging, Tempe, AZ). A homemade fluid cell was used and the AFM was operated in magnetic tapping mode (MAC) using MAC levers operated around their resonance frequency of 25 kHz (in water) with a force constant of $k_{MAClever} = 2.8$ N/m (nominal). The scan rate used for imaging was in the range of 1.2–1.9 Hz for all cases. The free amplitude for tapping mode imaging was in all cases at ~8.5 V, and the amplitude on scanning was ~6.5 V.

Differential scanning calorimetry (DSC)

Experiments using MLVs composed of the different lipid mixtures were performed in a Science Corp N-DSCII Calorimeter (Lindon, UT; for pure porcine brain ceramide) or a VP-DSC (MicroCal, Northampton, MA; for POPC/ceramide and POPC/ceramide/chol mixtures) at 8–20 mM total lipid concentration. The scan rate was 0.5 K/min versus pure water. Neither change in the total concentration nor in the scan rate gave significant changes in the obtained results.

Fourier transform infrared spectroscopy (FTIR) experiments

With the use of FTIR, the thermotropic phase behavior of deuterated POPC-d31 and nondeuterated ceramide in POPC-d31/ceramide mixtures can be measured independently. This process is done by monitoring the POPC-d31

CD_2 and ceramide CH_2 acyl-chain stretch modes as a function of temperature, which appears in different regions of the IR spectra. IR spectra were recorded on a Perkin-Elmer 2000 Fourier transform IR-spectrometer (Perkin-Elmer, Norwalk, CT) equipped with a liquid nitrogen-cooled Mercury/Cadmium/Telluride detector interfaced to a microcomputer with Spectrum 2000 software (Perkin-Elmer, Norwalk, CT). Five microliters of multilamellar vesicles sample (50 mg/ml lipid total concentration) were placed between two FTIR CaF_2 windows. The temperature was controlled by a Peltier device and monitored by a thermocouple placed on the FTIR window. Infrared spectra in the CH_2 stretching region from 3000 to 2800 cm^{-1} and CD_2 stretching region from 2200 to 2000 cm^{-1} were monitored as a function of temperature. Eight spectra were averaged at each temperature point. Spectra were continuously acquired at a temperature increase rate of 3°C/min. Phase transitions were determined by plotting the band positions of the CH_2 symmetric and CD_2 asymmetric stretch modes. The band positions were determined by taking the second derivative of the original spectra and averaging the band intercepts at 80% intensity.

RESULTS

POPC/ceramide mixtures

Giant vesicle experiments

LAURDAN GP images for GUVs composed of different POPC/ceramide mixtures were obtained at different temperatures. Fig. 2 *A* shows a representative example (POPC/ceramide 5:1 mol ratio). In this particular case, and above 36.5°C, the GUVs show an average low GP value characteristic of a fluid phase (29,30). At 36.5°C high GP regions corresponding to gel-like phase are clearly present in the GUVs. As the temperature is decreased the extent of high GP areas increases in the vesicle. In addition, the LAURDAN GP profile (obtained from the GP images) versus temperature
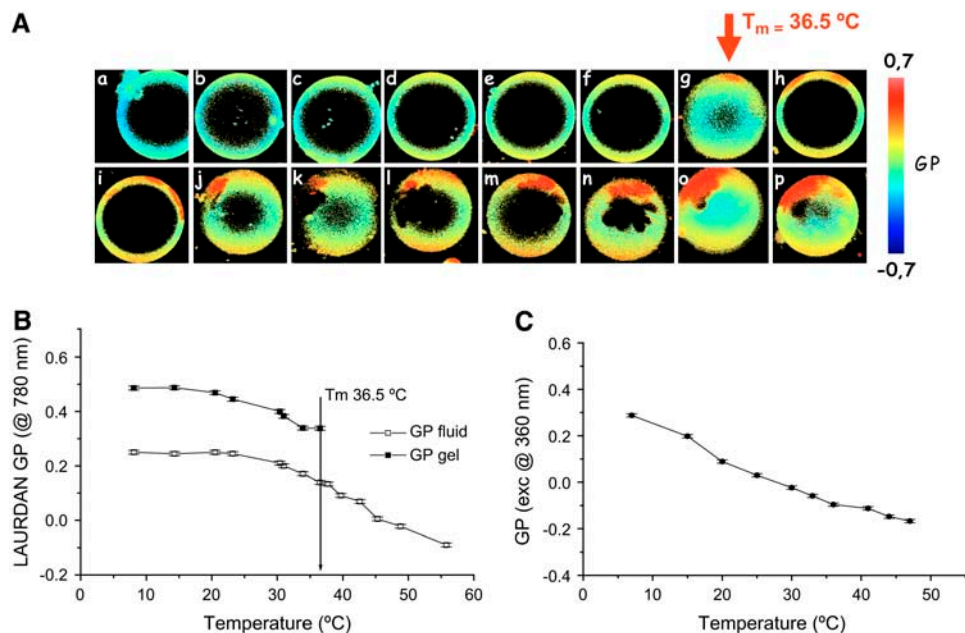

FIGURE 2 (*A*) Two-photon excitation GP images of LAURDAN-labeled GUVs composed of POPC/ceramide 5:1 mol/mol (false-color representation) as a function of temperature (*top panel*). The images have been taken either at the equatorial or polar regions of the GUV. The red areas correspond to the gel phase. The lack of signal in the polar region of the GUV (for the images taken at the GUV polar region) is due to the photoselection effect. The temperatures are: *a*, 58.5°C; *b*, 48.8°C; *c*, 45.3°C; *d*, 42.6°C; *e*, 39.7°C; *f*, 37.7°C; *g*, 36.5°C; *h*, 33.9°C; *i*, 31.0°C; *j*, 30.4°C; *k*, 23.2°C; *l*, 20.5°C; *m*, 14.3°C; *n*, 12.6°C; *o*, 10.3°C; and *p*, 8.1°C. (*B*) GP profile obtained at the level of single vesicles at different temperatures. GUV diameter is 30 μm. (*C*) LAURDAN GP versus temperature in multilamellar vesicles composed of POPC/ceramide 5:1 mol. No discontinuity at the phase transition of this mixture, determined from the LAURDAN GP experiments using GUVs (36.5°C), is observed in the bulk experiment in agreement with previous reported data (22).

is shown in Fig. 2 *B*. For comparative reasons, the LAURDAN GP values obtained from fluorescence cuvette experiments using multilamellar vesicles composed of POPC/ceramide (5:1 mol) at different temperatures is shown in Fig. 2 *C*. Although the LAURDAN GP bulk experiments indicate an overall decrease in the water dipolar relaxation process as the temperature is decreased (Fig. 2 *C*), no marked discontinuity was observed in the GP curve at the expected main phase transition temperature (~36–38°C for this mixture based on GUVs and also in DSC and IR experiments; see below). The LAURDAN GP temperature profile obtained in multilamellar vesicles is in agreement with that reported by Massey (22). From this LAURDAN GP profile Massey (22) concluded that no lipid phase coexistence is present in this mixture. Nevertheless, it is important to emphasize that the LAURDAN GP experiments under the two-photon microscope make it very clear that two different GP regions corresponding to the gel and fluid-like areas are present in the GUVs (see Fig. 2, *A* and *B*, for comparison). Fig. 3 *A* shows a series of different POPC/ceramide GUVs increasing the proportion of ceramide at room temperature

using DiI_{C18} and LAURDAN probes. The nonfluorescent region in the DiI_{C18}-labeled GUVs increases as the ceramide molar fraction increases and is indicative that the DiI_{C18} is segregated from the gel phase. This fact is directly observed in the fluorescent images obtained by using both probes simultaneously (see Materials and Methods; however, results are not shown) and further confirmed by comparing the DiI_{C18} fluorescent images with the LAURDAN GP images (Fig. 3 *A*). It is very important to note that the shape and size of the lipid domains are independent of the fluorescent probe used in the experiments. The last indicates that the presence of the fluorescent probes is not influencing the lateral pattern observed in the GUV's membrane. From the LAURDAN GP data shown in Fig. 3 it is clear that the vesicles display two different phases (gel- and fluid-disordered-like phases) in the different lipid mixtures at room temperature. Additionally, the nonfluorescent regions observed in the LAURDAN-labeled vesicles are due to the photoselection effect (23,24,35). This phenomenon is induced by a lack of excitation of the LAURDAN probe, particularly in the gel-like phase, due to the perpendicular orientation of the probe transition moment
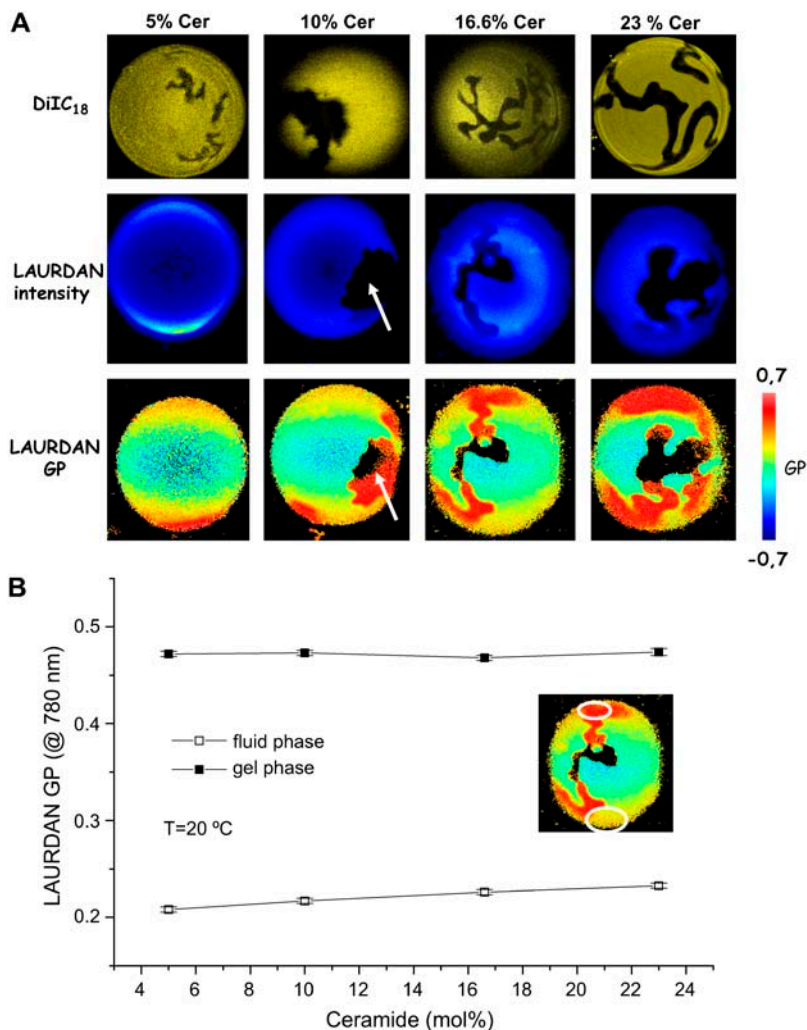

FIGURE 3 (*A*) Two-photon excitation fluorescence intensity and GP images of LAURDAN-labeled GUVs (*center* and *bottom panels*) and confocal images of DiI_{C18}-labeled GUVs (*top panel*) composed of POPC/ceramide 5:1 mol/mol (false-color representation) at 20°C. The images have been taken at the polar region of the GUV. The LAURDAN GP red areas correspond to the gel phase. The lack of intensity signal in the polar region of the GUV is due to the photoselection effect (indicated by the *white arrow* in the figure). Taking into account LAURDAN's information about phases, it is clear that the probe DiI_{C18} is segregated from the ceramide-rich gel phase (see text). The shape and size of the lipid domains are very similar using both probes (DiI_{C18} and LAURDAN), indicating that the presence of different probes is not affecting the lipid lateral structure. The GUV diameter is 30 μm. (*B*) Two-photon excitation GP profiles (gel and fluid membrane regions) of LAURDAN-labeled GUVs, increasing the ceramide molar fraction in the mixture (each GP point corresponds to an average of 10 vesicles). The temperature was 20°C. The inset shows the places where the GP function is normally taken in a GUV. These areas correspond, and are close to the center cross section of the vesicle, to discard GP variations due to the photoselection effect (23,24). The increment of the GP value in the fluid phase as the ceramide molar fraction increases is evident.

with respect to the plane of polarization of the excitation light (23,24,35). The photoselection effect observed for LAURDAN in the polar region of the vesicles confirms the fact that laterally ordered and disordered phases are present in the vesicles. Additionally, as it is observed in Fig. 3 *B*, the GP in the fluid phase increases as the ceramide fraction in the mixture increases. This trend indicates that the extent of the water dipolar relaxation process is diminishing in the fluid phase, a fact that can be interpreted as a slight increase of the lateral packing in this region of the membrane. This last effect is likely related to a gradual increase of the ceramide molar fraction in the POPC-rich fluid phase, suggesting partial miscibility of the lipid components in the mixture. In addition, the facts that dark areas are observed in the surface of the membrane and that the fluorescent probe is present in both leaflets of the bilayer (see Fig. 4) indicate that the gel phase domains span the lipid bilayer in agreement with previous observations done for other lipid mixtures (24,29,35).

AFM experiments

Using AFM, lipid domain coexistence in a broad temperature range was also observed in planar-supported membranes composed of different POPC/ceramide mixtures. The size and shape of the lipid domains were in good agreement with those found in the GUVs experiments. By combining AFM with fluorescence microscopy we observed that the probe DiI_{C18} was excluded from the flower/stripe domains corresponding to the observation in the GUVs experiments (Fig. 5). The height difference between the two phases observed in the AFM images (see Fig. 5) is 1.2 ± 0.1 nm, which is in agreement with previous AFM studies on coexisting fluid/gel membrane phases (38). Moreover the fluid/solid domain
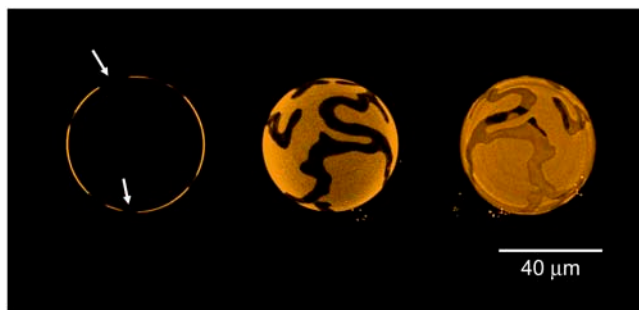

FIGURE 4 Gel lipid domains spanning the lipid bilayer (*white arrows*). Confocal fluorescence intensity image of DiI_{C18}-labeled GUV composed of POPC/ceramide (23 mol % ceramide) at the phase gel/fluid phase coexistence's temperature regime (false-color representation). The images correspond to the equatorial section of the GUV (*left*); the three-dimensional image of half of the vesicle (*center*); and the complete three-dimensional picture of the GUV (*right*). From the pictures, it is clear that in GUVs, gel domains in either monolayer are in register (because DiI_{C18} is present in both leaflets of the bilayer; see text).

regions also exhibit contrast in the AFM phase image, which is attributed to a difference in viscoelastic response between these regions. Taken together these observations all point to the conclusion that the observed domain pattern corresponds to coexisting fluid- and gel-like phases.

DSC and IR experiments

The DSC thermograms obtained for the different POPC/ceramide mixtures are shown in Fig. 6, *A* and *B*. The increase in the ceramide molar fraction in the lipid mixture causes two simultaneous effects:

1. A broadening and subsequent reduction of the area (enthalpy) of the low temperature endotherm (that corresponds to the POPC-rich areas) without substantial change in the main transition temperature.
2. A gradual contribution of a high temperature endotherm in the 20–50°C temperature range (likely corresponding to ceramide-rich domains).

This last peak shows a simultaneous temperature shift and broadening as the molar fraction of ceramide increases (see Fig. 6 *B* and Table 1). From this data it is evident that a broad gel/fluid phase coexistence temperature regime is present in the mixture, and it is very likely that a partial miscibility of the lipid components occurs in the mixture. Additionally, the main transition temperature observed for the high temperature endotherm in the DSC experiment corresponds very well to the temperature where gel phase areas are becoming visible in the GUVs experiments (see Table 1).

Fig. 6 *C* shows that it is possible to follow independently by using IR experiments the thermotropic behavior of each lipid component in the system (in this case, POPC and ceramide) by exploiting the different band positions of the CH_2 symmetric and CD_2 asymmetric stretch modes (ceramide and deuterated POPC, respectively). For the POPC/ceramide 5:1 mol mixture, ceramide shows a transition event at 37°C with a concurrent but smaller change in the CD_2 asymmetric stretch mode corresponding to deuterated POPC, suggesting that a fraction of POPC molecules are present in the ceramide-rich gel phase. This last data strongly supports a partial miscibility among the lipid components of the mixture in agreement with that observed in DSC and LAURDAN GP GUV experiments. Additionally, the tail-end of a second event involving POPC-d31 is observed at −5°C, which most likely corresponds to a gel/fluid phase transition of the POPC-enriched areas. This POPC transition appears at lower temperature than the low temperature thermal event observed by DSC (Fig. 5 *C*). This difference is explained by the fact that deuteration induces a reduction in the T_m of the POPC species of ~4°C (39). Overall, the results correlate well with the DSC data and confirm the presence of POPC-enriched fluid phase domains in coexistence with ceramide-enriched gel phase domains within a broad temperature regime.
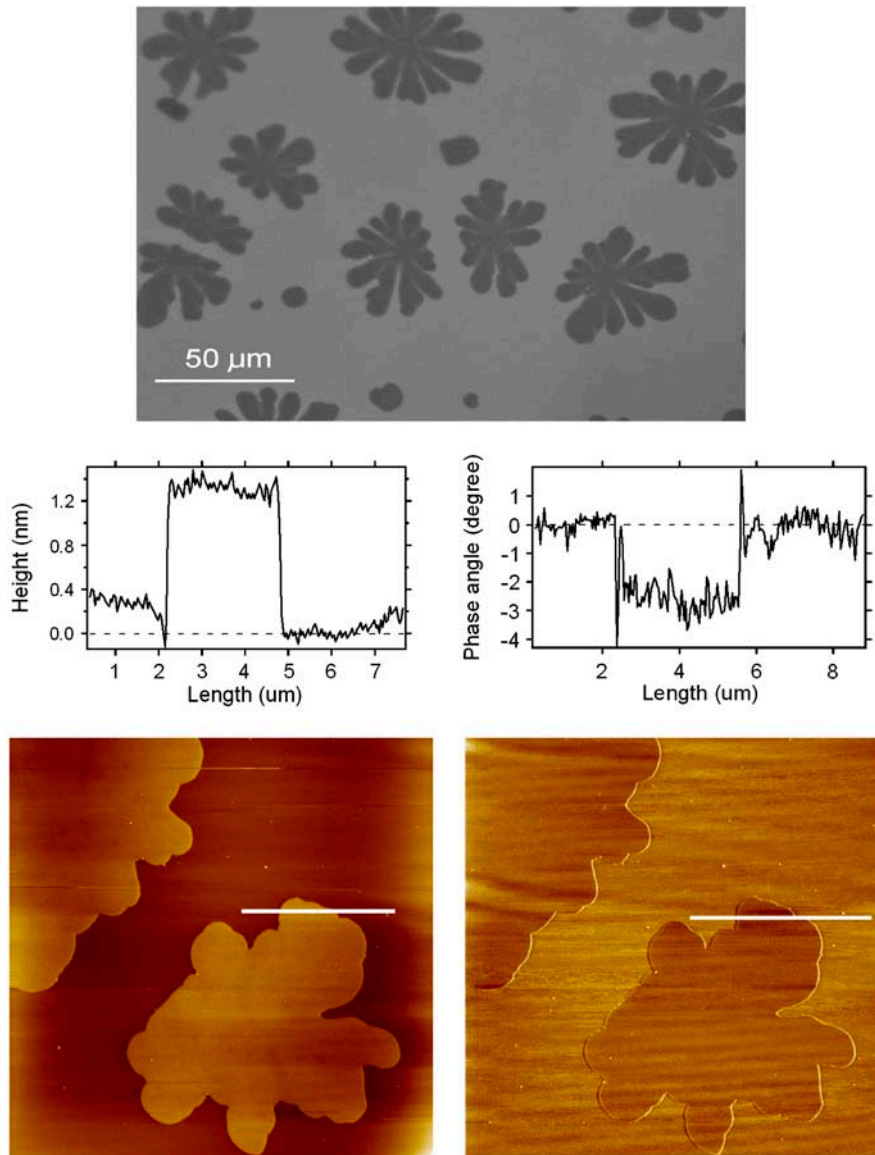
FIGURE 5   Fluorescence image (*top*) of a supported POPC/ceramide (5:1 mol ratio) membrane labeled with DiI_{C18}. The fluorescent probe is segregated from the flower-shaped domain regions. The AFM image shows (*bottom left*) that the nonfluorescent domains have an elevated height with respect to the surroundings (*center*). Phase imaging (*bottom right*) shows that the viscoelastic response is different between the observed areas.

POPC/ceramide/cholesterol mixtures

GUVs experiments

Addition of cholesterol produces changes in the lateral structure of the POPC/ceramide mixtures. For instance, for the POPC/ceramide 5:1 mol mixture at room temperature and above 5 mol % of cholesterol, the GP of the fluid phase progressively augments as the cholesterol molar fraction in the mixture increases (Fig. 7). For example, at ~20 mol % cholesterol, the GP value observed in the more fluid membrane region is to some extent lower than the one observed in the gel-like phase region (0.42 and 0.5, respectively; see Fig. 7), although two regions are still observed in the membrane. This last fact clearly indicates an ordering effect of cholesterol on the more fluid region of the membrane, diminishing the extent of water dipolar relaxation phenomena around the LAURDAN fluorescent probe. Additionally, the LAURDAN GP value observed after addition of 20 mol % of cholesterol in the more disordered regions of the membrane matches very well with the GP value reported for fluid-ordered phase at approximately the same temperature (25) and also agrees very well with the GP value obtained in GUVs composed of POPC/cholesterol (8:2 mol) at 20°C, where the liquid-ordered phase is present (data not shown). Remarkably, the observed domain shape from above 5 and up to 20 mol % of cholesterol in the POPC/ceramide mixtures is different from that observed in cholesterol containing ternary mixtures that display coexistence of fluid-ordered and fluid-disordered phases (25,40). In this last case, the presence of perfectly round domains is a characteristic of the fluid-ordered/fluid-disordered phase coexistence scenario, independent of the lipid composition, i.e., POPC/SM/chol,
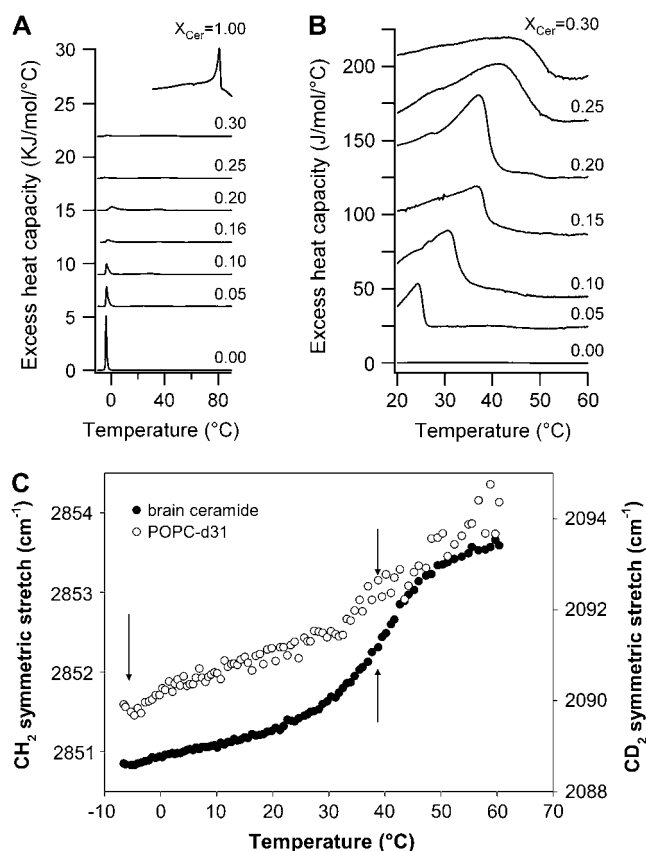
FIGURE 6 DSC thermograms of MLVs composed of different POPC/ceramide mixtures, including pure POPC and pure ceramide. (*A*) Complete scan from −10 to 90°C; (*B*) temperature range where the high-melting-temperature event occurs (the excess heat capacity is multiplied by a factor of 10 compared to *A*). (*C*) POPC-d31 CD_2 and ceramide CH_2 acyl-chain stretch modes obtained from the IR spectra of these lipids in the POPC-d31/ceramide (5:1 mol) mixture as a function of temperature. The arrows indicate the observed phase transition events in this mixture (see text). Notice that a fraction of POPC molecules undergoes a phase transition together with ceramide at 38°C.

DOPC/SM/chol, DOPC/DPPC/chol, pulmonary surfactant, and brush border membrane lipid extracts (8,25,40). When fluid domains are embedded in a fluid environment, circular domains will form because both phases are isotropic and the line energy (tension), which is associated with the rim of two demixing phases, is minimized by optimizing the area/perimeter ratio. This last signature (perfectly round domains) was not observed in the GUVs composed of POPC/ceramide/cholesterol mixtures explored in this work. On the other hand, no significant changes in the value of the LAURDAN GP function was observed in the ceramide-rich gel-like phase as the cholesterol content increases, indicating that the degree of dipolar relaxation processes in this phase is not affected in any significant way by the presence of cholesterol. It is important to note, however, that the temperature where lateral phase separation becomes apparent for the corresponding POPC/ceramide mixture (higher T_m, corresponding to the formation of ceramide-rich phases) decreases as the cholesterol molar fraction increases, in agreement with the DSC data (see below, Table 2). All these experiments indicate that the POPC/ceramide (5:1 mol) mixture with cholesterol concentrations from 5 and up to 20 mol % likely display coexistence of a gel- and fluid-ordered-like phases.

Above 22 mol % cholesterol a dramatic change is observed in the GUV membrane (see Fig. 8). Both probes, LAURDAN and DiI_{C18}, indicate the presence of three distinct regions in the lipid membrane: 1), a line-shaped region (LSR) that emits fluorescence (indicated by *arrows* in Fig. 11); 2), a fluorescent region (FR); and 3), a nonfluorescent region (NFR). A general feature in the images is the fact that the LSR appears to always surround the NFR. Additionally, the shape of the NFR is faceted and resembles a crystal-like structure. The LAURDAN GP data shows that the LSR and FR have high GP values (0.43 and 0.44, respectively) corresponding to a low extent of water dipolar relaxation processes around the fluorescent probe in the membrane. This last fact suggests that an ordered lateral lipid packing exists in both membrane regions (LSR and FR, see Fig. 8). Surprisingly, the fluorescence intensity in LSR is evident in the polar region of the vesicles where the LAURDAN photoselection effect is strong (Fig. 8 *B*), even though the LAURDAN GP value of the LSR is high. In general, high LAURDAN GP regions will display a strong photoselection effect on the polar regions of the vesicles, i.e., no fluorescence emission light is expected in these regions (24,35). The high fluorescence intensity observed at the polar region of the GUVs in the LSR regions appears to indicate that a reorientation of LAURDAN occurs in this particular membrane region. A corresponding high fluorescence intensity region (LSR) is also observed using DiI_{C18} probe (Fig. 8 *A*). These particular structures (appearing above 22 mol % and up to 30 mol % of cholesterol) disappear in the mixtures as the temperature is increased and reappear again at the same temperature upon cooling the samples. The fact that the formation of this particular lateral pattern is independent of the heating direction suggests absence of thermal hysteresis in the samples. Additionally, the temperature where these particular structures become visible agree very well with the higher T_m obtained using DSC and IR (see below, Table 2) for the same mixtures.

TABLE 1 Low/high transition temperatures obtained from the heat capacity profile of different POPC/ceramide MLVs; the temperature at which the lipid domains become visible in the GUV experiments is also indicated in the table

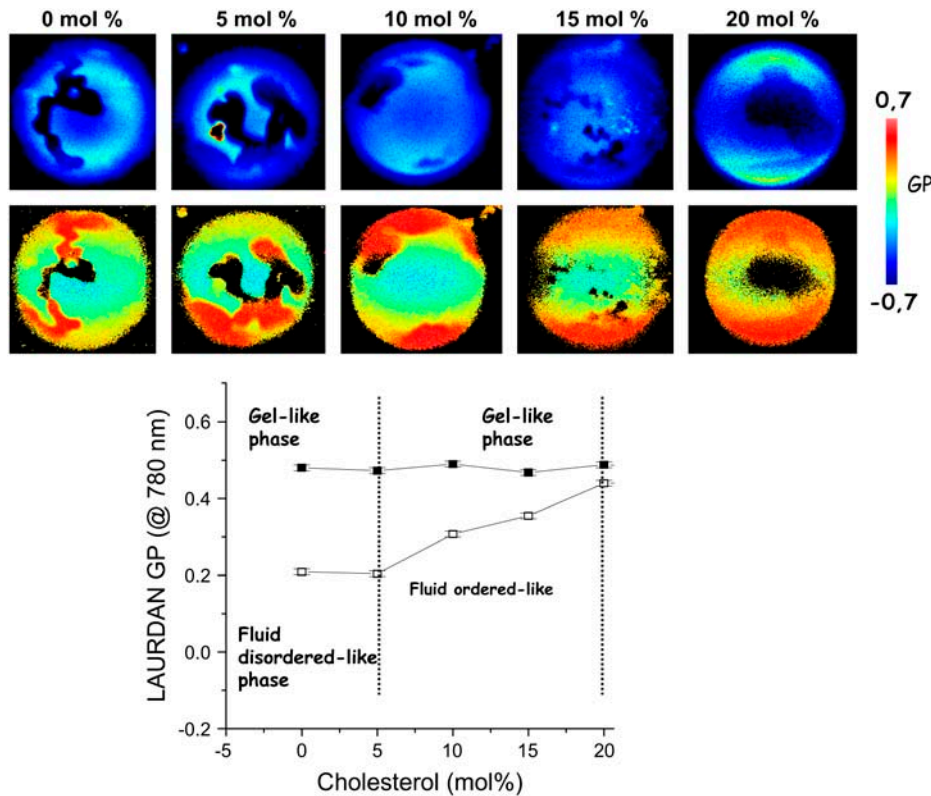| Mol % ceramides	T_{low} [°C]	T_{high} [°C]	T_{high} GUVs experiments [°C]
0	−3.7	—	—
5	−3.4	24.7	24.0
10	−3.4	30.3	31.0
15	−2.7	37.0	36.2
20	−0.7	37.3	38.0
25	−5.1	41.1	42.0
30	−3.1	43.5	—

FIGURE 7 Two-photon excitation GP and intensity images (*top*, false-color representation) of LAURDAN-labeled GUVs, with increasing the cholesterol molar fraction in the POPC/ceramide 5:1 mol mixture (each GP point corresponds to an average of 10 vesicles). The temperature was 20°C. The inset (*bottom*) shows the GP profile obtained in the microscopy experiment versus cholesterol concentration and the observed lipid phases. The increment of the GP value in the more disordered phase upon addition of cholesterol is evident.

DSC and IR experiments

DSC data for these mixtures are summarized in Fig. 9, *A* and *B*. Addition of cholesterol produces a decrease in the main transition temperature of the high melting peak (that correspond to the formation of ceramide-rich domains, see Table 2) and gradually abolishes the transition observed for the low melting peak (corresponding to the POPC-rich domains) for cholesterol concentrations between 5 and 30 mol %. For the POPC/ceramide (5:1) + 26 mol % of cholesterol the IR data show a transition temperature for the ceramide-rich fraction similar to that observed by DSC (23°C, see Fig. 9 *C* and Table 2). In the IR experiments the phase transition observed at 23°C for ceramide does not involve any significant participation of the POPC as was observed for the mixture without cholesterol (see Fig. 9 *C*). On

the other hand, the presence of cholesterol at 26 mol % abolishes the low melting temperature transition event that corresponds to the POPC-enriched membrane region.

AFM experiments

To further explore the particular lateral structure observed for POPC/ceramide (5:1 mol) containing 24–30 mol % of cholesterol, AFM images were obtained for supported membranes composed of POPC/ceramide (5:1 mol) with 15 and 26 mol % of cholesterol (Fig. 10). At 15 mol % cholesterol the system exhibits domain coexistence with a height difference between the domains of 7 Å (Fig. 10 *A*) in contrast to that observed for POPC/ceramide (5:1 mol) without cholesterol, where the height difference between the gel and fluid domains was ~12 Å. Above 22 mol % of cholesterol the lateral pattern of the membrane is very complex, showing a distribution of height differences between the laterally ordered and disordered domains (Fig. 10, *B* and *C*). Interestingly, exposure to methyl-β-cyclodextrin (that removes cholesterol from the membranes) restores the system to a configuration with domains corresponding to those observed for POPC/ceramide without cholesterol (Fig. 10 *D*).

DISCUSSION

POPC/ceramide mixtures

Our results from different experimental techniques clearly show that POPC/ceramide mixtures display coexistence of
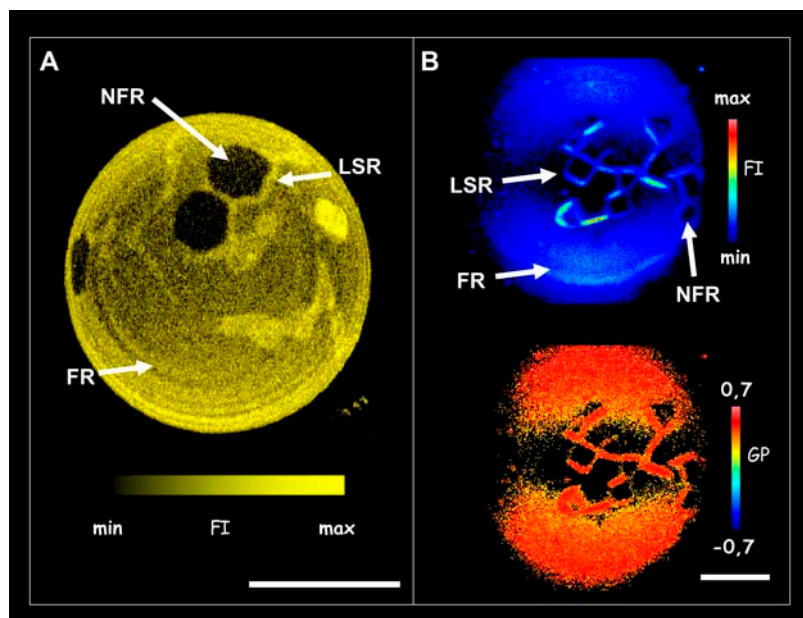
TABLE 2 Cholesterol content dependence of the low/high transition temperature obtained from the heat capacity profile of POPC/ceramide (5:1 mol) MLVs

Mol % cholesterol	T_{low} [°C]	T_{high} [°C]	T_{high} GUVs experiments [°C]
0	−2.7	37.0	36.5
5	−3.3	35.4	35.0
10	−2.3	34.7	33.8
15	−0.4	31.0	30.0
20	4.3	28.7	28.0
25	2.5	24.1	23.0
30	3.2	23.1	—

FIGURE 8 Confocal image of DiI$_{C18}$-labeled GUV (*A*), and two-photon excitation fluorescence intensity and GP images of a LAURDAN-labeled GUV (*B*) composed of (POPC/ceramide)/cholesterol (5:1)/26 mol % (false-color representation) at 20°C. The images have been taken at the polar region of the GUV. The indicated areas are line-shape region (*LSR*), fluorescence region (*FR*), and nonfluorescent region (*NFR*); see text. The white bars correspond to 15 μm.

gel and fluid phases, characterized by the presence of micron-sized gel domains with striped/flowerlike shapes in a broad range of compositions and temperatures, in contrast to that reported by Massey (22). Incorporation of ceramide clearly affects the lateral organization of the POPC interface even at low ceramide molar fraction (5 mol %) showing partial miscibility of the mixture's lipid components in the different lipid domains. This partial miscibility is reflected in the DSC experiments and LAURDAN GP images (Fig. 3 and Fig. 6, *A* and *B*) and further confirmed from the IR data (Fig. 6 *C*).

It is interesting to notice the agreement of our observation with that observed and reported for POPC/palmitoyl ceramide in the work of Hsueh et al. (21) . Even though we used porcine brain ceramide in our mixtures (porcine brain is a complex mixture of different ceramides, see Materials and Methods) the phase diagram reported by Hsueh et al. (21) agrees very well with the lateral features observed for the POPC/porcine brain ceramide mixtures in the temperature range explored in our experiments. This correlation is very interesting since it supports the idea that it is possible to establish a direct connection between compositionally complex and simple mixtures as was proposed previously in the literature (8,25, 37,41). Additionally, Hsueh et al. (21) also claim the presence of a metastable solid ceramide phase above 20 mol % of ceramide. By visual inspection of the GUVs composed of POPC/ceramide mixtures (up to 30 mol % of ceramide) the presence of a resolvable microscopic-sized third region in the membrane was not found either by using LAURDAN or DiI$_{C18}$. Nevertheless, it is important to stress that we cannot discard conclusively from the GUVs experiments the existence of this particular (metastable solid) phase, because

1. The size of these particular domains can be below the resolution of the microscope; or

2. If this phase is associated or included within the ceramide-rich gel phase, and assuming that the partition of the fluorescent probes is not affected by its presence, this phase will be invisible for these probes (DiI$_{C18}$ is excluded from the gel/solidlike phases while LAURDAN is present, but no differences will be expected in the water dipolar relaxation process between ceramide gel and solid phases).

However, the fact that no visible third region in the nanometer size range was detected in the planar membranes using AFM and no endotherm at high temperatures was detected in the DSC experiments (in particular, at ~80°C, which would reflect pure ceramide membranes) argues against the presence of this metastable solid phase for these particular mixtures in our experiments. It is fair to mention, however, that this particular difference may be related to the fact that we used a natural mixture of different ceramide species in our experiments, i.e., not a real binary mixture as Hsueh et al. (21) used.

We believe that one of the relevant issues in this study is the marriage between the morphological information of the membrane from the single vesicle/planar membrane experiments (using fluorescence microscopy/AFM) and techniques based on liposome solutions, which report on bulk mean parameters. As was pointed out in Introduction, above, bulk experiments per se may lack information that can be crucial to understanding the lateral organization of complex mixtures (8,41). In particular, LAURDAN GP experiments in cuvette and in the microscope show a clear example of the importance of correlating bulk parameters with morphological information to draw more realistic conclusions about the behavior of the system under study. As was reported previously (22) and also observed by us (Fig. 2 *C*), the measured
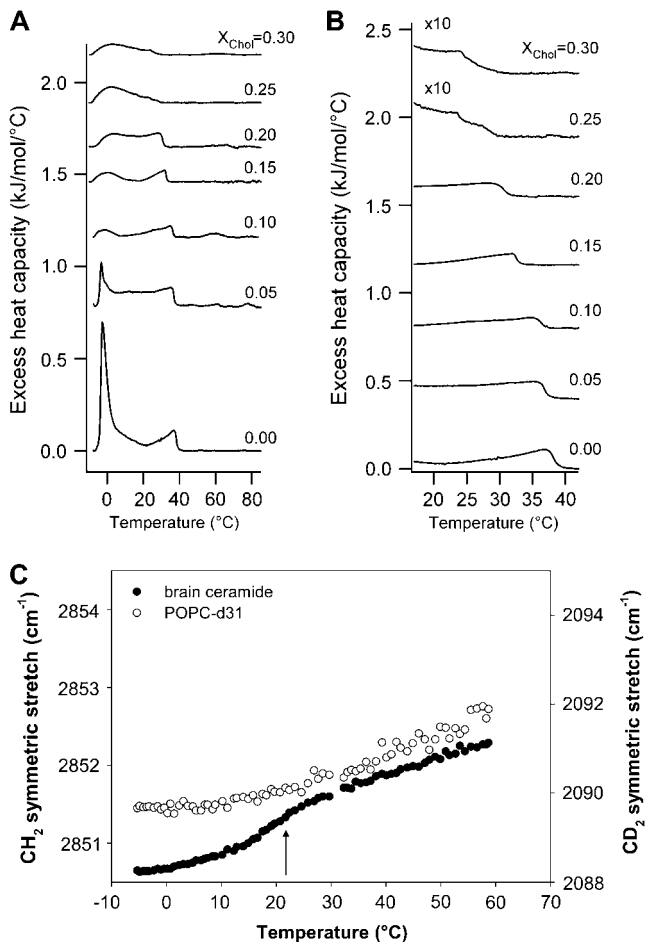
FIGURE 9 DSC thermograms of MLVs composed of POPC/ceramide (5:1 mol) + cholesterol at different molar fractions (from 0 to 30 mol %). (A) Complete scan from −10 to 90°C; (B) temperature range where the high-melting-temperature event occurs. Notice the shift to lower temperatures of the high-temperature endotherm as cholesterol concentration is increased. (C) POPC-d31 CD_2 and ceramide CH_2 acyl-chain stretch modes obtained from the IR spectra of these lipids in the POPC-d31/ceramide (5:1 mol) + 26 mol % cholesterol mixture as a function of temperature. The arrow indicates the observed phase-transition event in this mixture (see text). Notice the absence of phase-transition events observed for POPC in the mixture without cholesterol (compare with Fig. 5 C).

LAURDAN GP temperature profile for POPC/ceramide MLVs does not show any discontinuity at the temperature where the nucleation of gel phase is expected in contrast to that observed in the LAURDAN GP experiments using fluorescence microscopy (and also supported by AFM, DSC, and FTIR data). This apparent discrepancy can be explained by considering the additive property of the anisotropy function (42) that was based on the early observations of Gregorio Weber about the additive properties of the polarization function (43). The additive properties of the anisotropy function also applies to the LAURDAN GP function. For example, the average GP (GP_{av}) measured in the cuvette follows the form

$$GP_{av} = X_g GP_g + X_f GP_f, \qquad (2)$$

where GP_g and GP_f are the observed GP values for the gel and fluid phases, respectively, and X_g and X_f are factors that represent the fractional contribution of each lipid phase to the GP_{av}. In Eq. 2, the X factor primarily depends on the total area fraction of the gel and fluid phases and the probe concentration in each lipid phase. Since LAURDAN shows an even distribution in membranes displaying phase coexistence (24,35) we can assume that the X factor in Eq. 2 is mainly influenced by the area fraction of each lipid phase. It is important to remark that the relationship between the area fractions of the coexisting phases does not correspond with that observed between the molar fractions of the lipid species in the mixture since the molecular area of a lipid in the gel phase is almost one-third of that observed in the fluid phase. For example, if total immiscibility between the components of a binary mixture is considered, the contribution of the gel phase area will be always lower compared to that corresponding to the molar fraction of the high-melting-temperature lipid component. Taking into account this last effect, we can speculate that a significant contribution of the gel phase's area (high molar fraction of the high melting temperature lipid component) will be required in order to have an observable discontinuity in the bulk GP temperature profile at the phase transition temperature of the mixture. In our case, ceramide cannot be incorporated into the POPC membranes above 30 mol % (see Materials and Methods), and their mixtures with POPC exhibit phase transition events with low cooperativity and partial lipid miscibility. Taking into account Eq. 2 and the abovementioned facts, we predict that a negligible change in the bulk GP_{av} temperature profile will occur at the phase transition temperature of these mixtures (as observed in Fig. 2 C), even though gel lipid domains are being formed in the sample (as demonstrated by the fluorescence microscopy experiments). Additionally, the fact that the extent of water dipolar relaxation process decreases in the fluid phase as the temperature decreases (33) (see Fig. 2 C) will enhances the masking effect in the bulk experiments. A similar analysis can be drawn with regard to the lack of evidence for domain formation in POPC/ceramide mixtures based on DPH fluorescence anisotropy measurements (22). DPH probe, like LAURDAN, is known to be present at similar concentration in both lipid phases and the discussion stated above (additive property of the anisotropy function and lipid domain area fraction contribution) can also be applied for this particular case. Therefore, the hypothesis that similar length fatty acid chains between natural occurring ceramide and POPC lipids precludes gel/fluid phase coexistence (22) can no longer be sustained. Several articles in the literature (19–21) show gel/fluid phase coexistence in phospholipids (mainly PCs)/ceramide mixtures and this particular POPC/ceramide mixture is not an exception. It is our opinion that the fact that ceramide laterally segregates in POPC membranes is related to the nature of its small polar headgroup (with low hydration
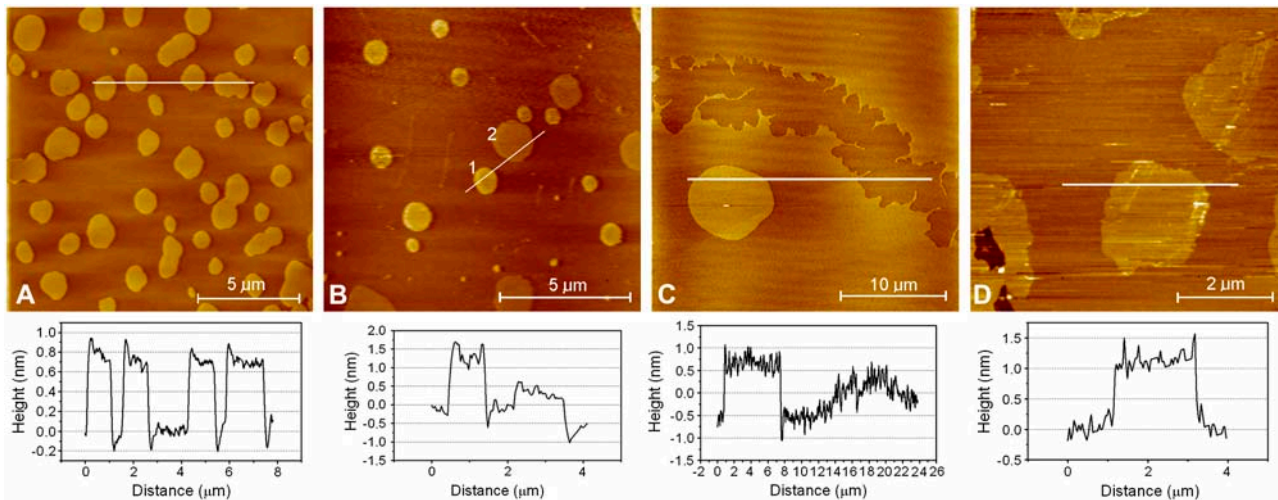
FIGURE 10 AFM images of the effect of cholesterol in membranes with the basic composition POPC/ceramide (5:1). Inclusion of 15 mol % cholesterol (*A*) in the supported membrane produces consistently uniform domains with a height difference between the domains and the surrounding membrane of 0.7 ± 0.1 nm. When increasing the cholesterol content to 26%, different domain types with characteristic heights are observed, as illustrated in panels *B* and *C*. Typical domain heights observed in this case are 1.2 ± 0.2 nm (type 1) and 0.6 ± 0.2 nm (type 2). (*D*) When cholesterol is removed with methyl-β-cyclodextrin from membranes with 26% cholesterol (10 mg/ml, 10 min), the system reverses to essentially the same domain height as observed without the presence of cholesterol (see also Fig. 6).

capacity) and the possibility for it to establish intermolecular hydrogen networks (21,44).

POPC/ceramide/cholesterol mixtures

One of the interesting issues in the experiments performed with this ternary mixture is the lack of fluid-ordered or fluid-disordered phase coexistence, as observed in mixtures containing other ceramide-based lipids (for example, sphingomyelin (25)). From our experiments we can observe that the effect of the cholesterol has two particular regimes (above and below 22 mol % of cholesterol for the POPC/ceramide 5:1 mol). Up to 20 mol % of cholesterol we observe that the fluid phase shows a gradual ordering effect. The LAURDAN GP values obtained in these last cases are in good agreement with GP values reported for fluid-ordered phases (25), suggesting that the fluid phase becomes more laterally ordered with increasing cholesterol molar fraction. This last fact is supported by the progressive broadening of the low melting transition endotherm (POPC-rich domains) as cholesterol concentration augments in the DSC experiments, and the decrease in the height differences between these two regions in the AFM experiments (Fig. 10), as is expected for a fluid ordered-gel phase coexistence. On the other hand, the cholesterol effect in the gel-like phase regions is characterized by a decrease in the higher transition temperature of almost 10°C (for 20 mol % cholesterol), with respect to the sample without cholesterol showing no changes in either the hydration properties of the membrane interface (the LAURDAN GP value remains constant in these membrane regions) or the domain shape. We speculate

that the reduction in the higher transition temperature may be explained by changes in the ordered domain's lipid composition induced by the presence of cholesterol. Additionally, and in contrast to that observed in membranes displaying liquid immiscibility (8,25), the absence of perfectly round domains in the POPC/ceramide/cholesterol mixture supports the idea of a persistence of a phase-separated ceramide-rich gel-like phase up to 20 mol % of cholesterol. Therefore, we conclude that a coexistence of gel-like and fluid-ordered-like phases coexists at room temperature in the POPC/ceramide (5:1 mol) mixtures containing 5–20 mol % cholesterol. This observation supports the idea that ceramide induces a particular lateral organization distinct from those proposed in the raft hypothesis. Although the mixture we use in our experiment is far away from the compositionally complex situation of a biological membrane (but also far from the case of a two- or three-component model system), we believe that it is fair to speculate that this phenomenon could take part in biologically relevant situations. For instance, the presence of gel-like phase regions may cause strong changes in the membrane's physical properties as happens in apoptosis (2).

A very complex membrane lateral pattern is observed above 22 mol % of cholesterol in the POPC/ceramide 5:1 mol mixture. In the GUV experiments, three different regions are observed in these membranes (LSR, FR, and NFR; see Fig. 11). In particular, the information given by LAURDAN through the photoselection effect is very valuable and interesting to comment on. The photoselection effect is sketched in Fig. 11. Considering a circular polarization in the excitation light confined in the *x,y* plane, by exploring different regions of a spherical vesicle (at a

given vertical section), strong excitation occurs in the regions where LAURDAN's transition moment is aligned parallel to the polarization plane of the excitation light, i.e., the equatorial region of the vesicle (23,24,35). In other words, when observing the polar region of a spherical lipid vesicle we will find lower excitation compared with that obtained at the equatorial region of the vesicle (23,24,35). In addition, this last fact depends on the phase state of the lipids. Observing a single-component lipid vesicle at the polar region we obtain large differences in the fluorescent intensity values if the images correspond to disordered (Fig. 11 A) and ordered lipid phases (Fig. 11 B). In an ordered lipid phase such as the gel phase (Fig. 11 B), the packing of the lipid molecules is very tight, preventing wobbling of the fluorescent probe (notice that LAURDAN's transition moment is aligned parallel to the lipid hydrophobic chains). Since the excitation efficiency is proportional to the cosine squared of the angle between the transition moment of the probe and the polarization plane of the excitation light (the angle is close to 90° in this case) the excitation efficiency of LAURDAN molecules in a gel phase membrane is very low. Instead, in the disordered phase we always have a component of LAURDAN's transition moment parallel to the excitation light polarization plane because of the relatively low lipid order (Fig. 11 A). This last fact allows more efficient LAURDAN excitation in the disordered lipid phase when gel/fluid phase coexistence is present; see Figs. 2, 3, and 6 (23,24,35). To explain the fact that the LSR is observable in the photoselection region (polar part of the GUV), the transition moment of LAURDAN probe in this membrane region must be either parallel or tilted <90°, in respect to the membrane surface plane (Fig. 11 C, notice that the maximum of efficiency will occur when the transition moment is

parallel to the polarization plane, which is oriented in the x,y plane parallel to the membrane surface). Importantly, LSR has high GP values, indicating that a tight lipid lateral packing is present in this particular membrane region. A similar case was also observed in bovine lipid extract surfactant below 20°C, where two solidlike phases coexisted, and one was tilted (37). The LAURDAN GP value for the FR strongly favors the idea of an additional ordered phase being present in the membrane (most likely a liquid-ordered phase). In this last case, the photoselection effect operates as expected (see Fig. 8, GP image, left side of GUV). Therefore, the main difference between LSR and FR will be the LAURDAN orientation that can be related with the lipid orientation in the membrane. Additionally, the particular shape of the NFR suggests a crystalline packing of the lipids, although no fluorescent parameters are in hand to further evaluate this last hypothesis. The NFR could correspond to crystalline domains composed of pure lipid species (for instance, ceramide or cholesterol), but no signatures of high temperature melting events (such as those for pure ceramide or cholesterol crystals) were observed in the DSC data to fully support this hypothesis. In addition, the fact that a nonfluorescent region is present in the membrane, is unexpected using LAURDAN, since in general this probe is homogeneously distributed in the membranes displaying phase coexistence (gel/fluid, fluid-ordered/fluid-disordered) (24,35). AFM data also shows that addition of cholesterol concentration above 22 mol % changes the physical characteristics of the membrane compared to those observed below 20 mol %. In particular, at 26 mol % of cholesterol, the height differences among the gel-like lipid domains and the lower membrane regions observed in the AFM images (Fig. 10) show distributed values and a variety of different
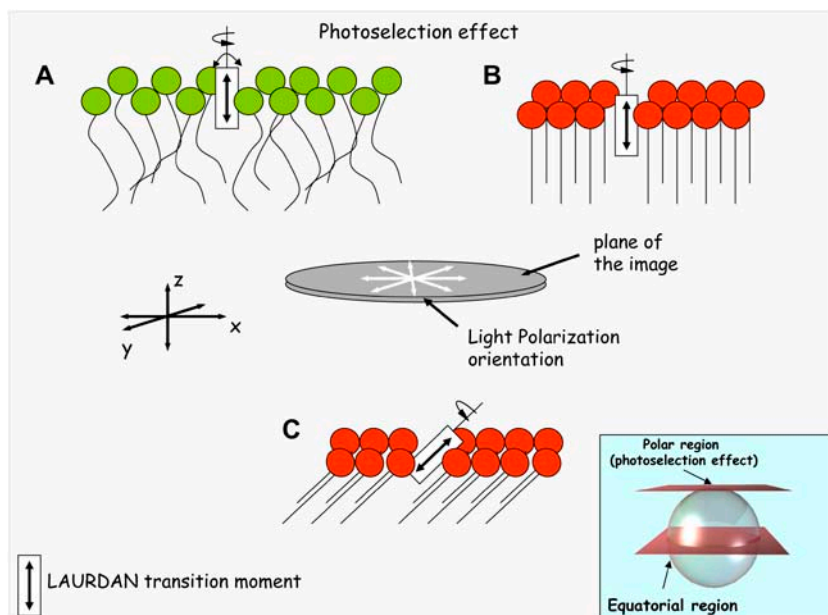

FIGURE 11 Schematic representation of the photoselection effect using circular polarized-excitation light that occurs at the polar region of the GUV. The double-headed curved arrows associated with the LAURDAN transition moment in the fluid phase (A) denote probe mobility (wobbling), which dramatically decreases in the gel phase (B). The difference in probe mobility explains why the fluorescence intensity coming from the fluid phase in the photoselection region (polar region of the GUVs) is considerably higher than that observed in the gel phase. (C) Possible configuration of the LSR observed in Fig. 11. The inset shows the polar and equatorial regions of the vesicle.

domain shapes. Interestingly, this effect is reverted upon cholesterol extraction, since the height difference between the lipid phases returns to the 1.2-nm value observed for gel/fluid phase coexistence where cholesterol is absent in the mixture. Taking into account the compositional heterogeneity of porcine brain ceramide (see Materials and Methods), a lateral redistribution of these lipid species in presence of high amounts of cholesterol can explain the particular membrane pattern observed in the AFM and fluorescence microscopy experiments. At this point it is clear that a detailed model to explain this particular complex lateral structure (generated upon addition of 22 mol % of cholesterol to the POPC/ceramide 5:1 mol mixture) is still far from being obtained. However, we feel that local lipid domain compositional information would be crucial to comprehend this phenomenon. We assume that the dramatic change in the membrane lateral pattern above this critical cholesterol concentration can be explained, as was mentioned above, by considering a marked redistribution of the different lipid molecular species in the lateral plane of the membrane. In line with this idea, Megha and London (18) reported that ceramide displaces cholesterol from ordered lipid domains. As was demonstrated by these authors (18), these two lipid species compete with each other to be included in ordered-like phases. However, there are other plausible hypotheses that may explain the complex lateral membrane pattern observed when cholesterol concentration is above 22–24 mol % in the POPC/ceramide (5:1 mol) mixture, namely:

1. The presence of many different ceramide species (different fatty acid compositions) can be responsible for the presence of multiple types of lipid domains, simply by speculating that the different ceramides can show particular interaction with the other lipid components of the mixture (something that is currently tested in our laboratory using mixtures containing a single ceramide species).

2. The presence of the ceramide channels (45) in our mixture may explain the particular lateral pattern, in particular the presence of LSR with unusual photoselection properties.

If ceramide molecules organize perpendicular to the normal of the membrane as was proposed by Siskind et al. (45), and assuming that LAURDAN is located parallel to the lipid hydrophobic chains, a strong excitation in the photoselection region (polar part of the vesicle) would be expected. Presence of cholesterol and unsaturated phospholipids, as happens in our mixtures, is required to generate this particular structure (15). To further explore this possibility, leakage experiments are currently being performed in our laboratory based on the new protocol described by Ambroggio et al. (46,47) using GUVs. Finally, it is important to point out that the three regions observed in the membranes were not exclusively generated by cholesterol. By adding ergosterol to the same POPC/ceramide mixture (data not shown) we

observe a similar phenomenon to that obtained for cholesterol. Interesting enough, addition of the sterol lanosterol does not produce this particular lateral pattern. The ergosterol concentration needed to induce these three distinct regions in the membrane was ~15 mol %, lower than that the 22 mol % observed for cholesterol. Additionally, binary mixtures of phospholipids and ergosterol was reported to show a very similar phase diagram to that observed in phospholipids/cholesterol mixtures (48).

REFERENCES

1. Kolesnick, R. N., F. M. Goni, and A. Alonso. 2000. Compartmentalization of ceramide signaling: physical foundations and biological effects. *J. Cell. Physiol.* 184:285–300.

2. van Blitterswijk, W. J., A. H. van der Luit, R. J. Veldman, M. Verheij, and J. Borst. 2003. Ceramide: second messenger or modulator of membrane structure and dynamics? *Biochem. J.* 369:199–211.

3. Norlen, L. 2001. Skin barrier structure and function: the single gel phase model. *J. Invest. Dermatol.* 117:830–836.

4. Bouwstra, J. A., P. L. Honeywell-Nguyen, G. S. Gooris, and M. Ponec. 2003. Structure of the skin barrier and its modulation by vesicular formulations. *Prog. Lipid Res.* 42:1–36.

5. Hill, J. R., and P. W. Wertz. 2003. Molecular models of the intercellular lipid lamellae from epidermal stratum corneum. *Biochim. Biophys. Acta.* 1616:121–126.

6. Shah, J., J. M. Atienza, R. I. Duclos, Jr., A. V. Rawlings, Z. Dong, and G. G. Shipley. 1995. Structural and thermotropic properties of synthetic C16:0 (palmitoyl) ceramide: effect of hydration. *J. Lipid Res.* 36:1936–1944.

7. Bagatolli, L. A., E. Gratton, and G. D. Fidelio. 1998. Water dynamics in glycosphingolipid aggregates studied by LAURDAN fluorescence. *Biophys. J.* 75:331–341.

8. Bernardino de la Serna, J., J. Perez-Gil, A. C. Simonsen, and L. A. Bagatolli. 2004. Cholesterol rules: direct observation of the coexistence of two fluid phases in native pulmonary surfactant membranes at physiological temperatures. *J. Biol. Chem.* 279:40715–40722.

9. Sot, J., F. J. Aranda, M. I. Collado, F. M. Goni, and A. Alonso. 2005. Different effects of long- and short-chain ceramides on the gel-fluid and lamellar-hexagonal transitions of phospholipids: a calorimetric, NMR, and x-ray diffraction study. *Biophys. J.* 88:3368–3380.

10. Veiga, M. P., J. L. Arrondo, F. M. Goni, and A. Alonso. 1999. Ceramides in phospholipid membranes: effects on bilayer stability and transition to nonlamellar phases. *Biophys. J.* 76:342–350.

11. Holopainen, J. M., M. I. Angelova, and P. K. Kinnunen. 2000. Vectorial budding of vesicles by asymmetrical enzymatic formation of ceramide in giant liposomes. *Biophys. J.* 78:830–838.

12. Cremesti, A. E., F. M. Goni, and R. Kolesnick. 2002. Role of sphingomyelinase and ceramide in modulating rafts: do biophysical properties determine biologic outcome? *FEBS Lett.* 531:47–53.

13. Futerman, A. H., and Y. A. Hannun. 2004. The complex life of simple sphingolipids. *EMBO Rep.* 5:777–782.

14. Goni, F. M., and A. Alonso. 2002. Sphingomyelinases: enzymology and membrane activity. *FEBS Lett.* 531:38–46.

15. Siskind, L. J., and M. Colombini. 2000. The lipids C2- and C16-ceramide form large stable channels. Implications for apoptosis. *J. Biol. Chem.* 275:38640–38644.

16. Siskind, L. J., R. N. Kolesnick, and M. Colombini. 2002. Ceramide channels increase the permeability of the mitochondrial outer membrane to small proteins. *J. Biol. Chem.* 277:26796–26803.

17. Xu, X., R. Bittman, G. Duportail, D. Heissler, C. Vilcheze, and E. London. 2001. Effect of the structure of natural sterols and sphingolipids on the formation of ordered sphingolipid/sterol domains (rafts). Comparison of cholesterol to plant, fungal, and disease-associated sterols and comparison of sphingomyelin, cerebrosides, and ceramide. *J. Biol. Chem.* 276:33540–33546.

18. Megha, and E. London. 2004. Ceramide selectively displaces cholesterol from ordered lipid domains (rafts): implications for lipid raft structure and function. *J. Biol. Chem.* 279:9997–10004.

19. Carrer, D. C., and B. Maggio. 1999. Phase behavior and molecular interactions in mixtures of ceramide with dipalmitoylphosphatidylcholine. *J. Lipid Res.* 40:1978–1989.

20. Holopainen, J. M., J. Lemmich, F. Richter, O. G. Mouritsen, G. Rapp, and P. K. Kinnunen. 2000. Dimyristoylphosphatidylcholine/C16:0-ceramide binary liposomes studied by differential scanning calorimetry and wide- and small-angle x-ray scattering. *Biophys. J.* 78:2459–2469.

21. Hsueh, Y. W., R. Giles, N. Kitson, and J. Thewalt. 2002. The effect of ceramide on phosphatidylcholine membranes: a deuterium NMR study. *Biophys. J.* 82:3089–3095.

22. Massey, J. B. 2001. Interaction of ceramides with phosphatidylcholine, sphingomyelin and sphingomyelin/cholesterol bilayers. *Biochim. Biophys. Acta.* 1510:167–184.

23. Bagatolli, L. A. 2003. Thermotropic behavior of lipid mixtures studied at the level of single vesicles: giant unilamellar vesicles and two-photon excitation fluorescence microscopy. *Methods Enzymol.* 367:233–253.

24. Bagatolli, L. A., and E. Gratton. 2001. Direct observation of lipid domains in free-standing bilayers using two-photon excitation fluorescence microscopy. *J. Fluor.* 11:141–160.

25. Dietrich, C., L. A. Bagatolli, Z. N. Volovyk, N. L. Thompson, M. Levi, K. Jacobson, and E. Gratton. 2001. Lipid rafts reconstituted in model membranes. *Biophys. J.* 80:1417–1428.

26. Angelova, M. I., S. Soleau, P. Meleard, J. F. Faucon, and P. Bothorel. 1992. Preparation of giant vesicles by external AC fields. Kinetics and application. *Prog. Colloid Polym. Sci.* 89:127–131.

27. Simonsen, A. C., and L. A. Bagatolli. 2004. Structure of spin-coated lipid films and domain formation in supported membranes formed by hydration. *Langmuir.* 20:9720–9728.

28. Bagatolli, L. A., and E. Gratton. 1999. Two-photon fluorescence microscopy observation of shape changes at the phase transition in phospholipid giant unilamellar vesicles. *Biophys. J.* 77:2090–2101.

29. Bagatolli, L. A., and E. Gratton. 2000. Two photon fluorescence microscopy of coexisting lipid domains in giant unilamellar vesicles of binary phospholipid mixtures. *Biophys. J.* 78:290–305.

30. Bagatolli, L. A., and E. Gratton. 2000. A correlation between lipid domain shape and binary phospholipid mixture composition in free standing bilayers: a two-photon fluorescence microscopy study. *Biophys. J.* 79:434–447.

31. Sanchez, S. A., L. A. Bagatolli, E. Gratton, and T. L. Hazlett. 2002. A two-photon view of an enzyme at work: *Crotalus atrox* venom PLA2 interaction with single-lipid and mixed-lipid giant unilamellar vesicles. *Biophys. J.* 82:2232–2243.

32. Parasassi, T., E. Kranowska, L. A. Bagatolli, and E. Gratton. 1998. LAURDAN and Prodan as polarity-sensitive fluorescent membrane probes. *J. Fluor.* 8:365–373.

33. Parasassi, T., G. De Stasio, A. d'Ubaldo, and E. Gratton. 1990. Phase fluctuation in phospholipid membranes revealed by LAURDAN fluorescence. *Biophys. J.* 57:1179–1186.

34. Parasassi, T., G. De Stasio, G. Ravagnan, R. M. Rusch, and E. Gratton. 1991. Quantitation of lipid phases in phospholipid vesicles by the generalized polarization of LAURDAN fluorescence. *Biophys. J.* 60:179–189.

35. Bagatolli, L. A. 2003. Direct observation of lipid domains in free-standing bilayers: from simple to complex lipid mixtures. *Chem. Phys. Lipids.* 122:137–145.

36. Bagatolli, L., E. Gratton, T. K. Khan, and P. L. Chong. 2000. Two-photon fluorescence microscopy studies of bipolar tetraether giant liposomes from thermoacidophilic archaebacteria *Sulfolobus acidocaldarius*. *Biophys. J.* 79:416–425.

37. Nag, K., J. S. Pao, R. R. Harbottle, F. Possmayer, N. O. Petersen, and L. A. Bagatolli. 2002. Segregation of saturated chain lipids in pulmonary surfactant films and bilayers. *Biophys. J.* 82:2041–2051.

38. Burns, A. R. 2003. Domain structure in model membrane bilayers investigated by simultaneous atomic force microscopy and fluorescence imaging. *Langmuir.* 19:8358–8363.

39. Leidy, C., W. F. Wolkers, K. Jorgensen, O. G. Mouritsen, and J. H. Crowe. 2001. Lateral organization and domain formation in a two-component lipid membrane system. *Biophys. J.* 80:1819–1828.

40. Veatch, S. L., and S. L. Keller. 2005. Seeing spots: complex phase behavior in simple membranes. *Biochim. Biophys. Acta.* 1746:172–185.

41. Gaus, K., E. Gratton, E. P. Kable, A. S. Jones, I. Gelissen, L. Kritharides, and W. Jessup. 2003. Visualizing lipid structure and raft domains in living cells with two-photon microscopy. *Proc. Natl. Acad. Sci. USA.* 100:15554–15559.

42. Jameson, D. M., and W. H. Sawyer. 1995. Fluorescence anisotropy applied to biomolecular interactions. *Methods Enzymol.* 246:283–300.

43. Weber, G. 1952. Polarization of the fluorescence of macromolecules. I. Theory and experimental method. *Biochem. J.* 51:145–155.

44. Huang, H. W., E. M. Goldberg, and R. Zidovetzki. 1999. Ceramides modulate protein kinase C activity and perturb the structure of phosphatidylcholine/phosphatidylserine bilayers. *Biophys. J.* 77:1489–1497.

45. Siskind, L. J., A. Davoody, N. Lewin, S. Marshall, and M. Colombini. 2003. Enlargement and contracture of C2-ceramide channels. *Biophys. J.* 85:1560–1575.

46. Ambroggio, E., F. Separovic, B. John, G. D. Fidelio, and L. A. Bagatolli. 2005. Direct visualization of membrane leakage induced by the antibiotic peptides: maculatin, citropin, and aurein. *Biophys. J.* 89:1874–1881.

47. Ambroggio, E. E., D. H. Kim, F. Separovic, C. J. Barrow, K. J. Barnham, L. A. Bagatolli, and G. D. Fidelio. 2005. Surface behavior and lipid interaction of Alzheimer β-amyloid peptide 1–42: a membrane-disrupting peptide. *Biophys. J.* 88:2706–2713.

48. Hsueh, Y. W., K. Gilbert, C. Trandum, M. Zuckermann, and J. Thewalt. 2005. The effect of ergosterol on dipalmitoylphosphatidylcholine bilayers: a deuterium NMR and calorimetric study. *Biophys. J.* 88:1799–1808.